Inorg. Chem. **2003**, *42*, 6447−6457

Modeling Features of the Non-Heme Diiron Cores in O_2-Activating Enzymes through the Synthesis, Characterization, and Oxidation of 1,8-Naphthyridine-Based Complexes

Jane Kuzelka,[†] Sumitra Mukhopadhyay,[†] Bernhard Spingler,[‡] and Stephen J. Lippard*,[†]

Department of Chemistry, Massachusetts Institute of Technology, Cambridge, Massachusetts 02139 and Institute of Inorganic Chemistry, University of Zürich, CH-8057 Zürich, Switzerland

Received May 30, 2003

Multidentate naphthyridine-based ligands were used to prepare a series of diiron(II) complexes. The compound $[Fe_2(BPMAN)(\mu\text{-}O_2CPh)_2](OTf)_2$ (**1**), where BPMAN = 2,7-bis[bis(2-pyridylmethyl)aminomethyl]-1,8-naphthyridine, exhibits two reversible oxidation waves with $E_{1/2}$ values at +310 and +733 mV vs Cp_2Fe^+/Cp_2Fe, as revealed by cyclic voltammetry. Reaction with O_2 or H_2O_2 affords a product with optical and Mössbauer properties that are characteristic of a (μ-oxo)diiron(III) species. The complexes $[Fe_2(BPMAN)(\mu\text{-}OH)(\mu\text{-}O_2CAr^{Tol})](OTf)_2$ (**2**) and $[Fe_2(BPMAN)(\mu\text{-}OMe)(\mu\text{-}O_2CAr^{Tol})](OTf)_2$ (**3**) were synthesized, where $Ar^{Tol}CO_2^-$ is the sterically hindered ligand 2,6-di(*p*-tolyl)benzoate. Compound **2** has a reversible redox wave at +11 mV, and both **2** and **3** react with O_2, via a mixed-valent Fe(II)Fe(III) intermediate, to give final products that are also consistent with (μ-oxo)diiron(III) species. The paddle-wheel compound $[Fe_2(BBAN)(\mu\text{-}O_2CAr^{Tol})_3](OTf)$ (**4**), where BBAN = 2,7-bis(*N*,*N*-dibenzylaminomethyl)-1,8-naphthyridine, reacts with dioxygen to yield benzaldehyde via oxidative *N*-dealkylation of a benzyl group on BBAN, an internal substrate. In the presence of bis(4-methylbenzyl)amine, the reaction also produces *p*-tolualdehyde, revealing oxidation of an external substrate. A structurally related compound, $[Fe_2(BEAN)(\mu\text{-}O_2CAr^{Tol})_3](OTf)$ (**5**), where BEAN = 2,7-bis(*N*,*N*-diethylaminomethyl)-1,8-naphthyridine, does not undergo *N*-dealkylation, nor does it facilitate the oxidation of bis(4-methylbenzyl)amine. The contrast in reactivity of **4** and **5** is attributed to a difference in accessibility of the substrate to the diiron centers of the two compounds. The Mössbauer spectroscopic properties of the diiron(II) complexes were also investigated.

Introduction

Carboxylate-bridged non-heme diiron centers occur in an important class of metalloproteins that react with dioxygen to effect a variety of essential chemical transformations.[1−4] Well-studied members of this family of proteins include hemerythrin (Hr), the hydroxylase component of soluble methane monooxygenase (sMMOH), the R2 subunit of ribonucleotide reductase (RNR-R2), and Δ-9 desaturase (Δ9D). The diiron core structures of these proteins in their reduced states are illustrated in Chart 1. Although these biological units all contain a carboxylate-bridged dimetallic motif, their functions vary dramatically. The protein Hr, found in certain marine invertebrates, reversibly binds dioxygen,[5] whereas some methanotrophs utilize the enzyme sMMOH to oxidize CH_4 to CH_3OH in the first step of the carbon metabolic pathway.[6] DNA biosynthesis is initiated by RNR-R2 through the generation of a tyrosyl radical,[7,8] and Δ9D produces a double bond in a saturated fatty acid.[9,10] Diiron components have also been identified at the active

* To whom correspondence should be addressed. E-mail: lippard@lippard.mit.edu.
[†] Massachusetts Institute of Technology.
[‡] University of Zürich.

(1) (a) Du Bois, J.; Mizoguchi, T. J.; Lippard, S. J. *Coord. Chem. Rev.* **2000**, *200−202*, 443−485. (b) Tolman, W. B.; Que, L., Jr. *J. Chem. Soc., Dalton Trans.* **2002**, 653−660.
(2) Solomon, E. I.; Brunold, T. C.; Davis, M. I.; Kemsley, J. N.; Lee, S.-K.; Lehnert, N.; Neese, F.; Skulan, A. J.; Yang, Y.-S.; Zhou, J. *Chem. Rev.* **2000**, *100*, 235−349.
(3) Wallar, B. J.; Lipscomb, J. D. *Chem. Rev.* **1996**, *96*, 2625−2657.
(4) Feig, A. L.; Lippard, S. J. *Chem. Rev.* **1994**, *94*, 759−805.
(5) Stenkamp, R. E. *Chem. Rev.* **1994**, *94*, 715−726.
(6) Merkx, M.; Kopp, D. A.; Sazinsky, M. H.; Blazyk, J. L.; Müller, J.; Lippard, S. J. *Angew. Chem., Int. Ed.* **2001**, *40*, 2782−2807.
(7) Stubbe, J.; van der Donk, W. A. *Chem. Rev.* **1998**, *98*, 705−762.
(8) Logan, D. T.; Su, X.-D.; Åberg, A.; Regnström, K.; Hajdu, J.; Eklund, H.; Nordlund, P. *Structure* **1996**, *4*, 1053−1064.
(9) Yang, Y.-S.; Broadwater, J. A.; Pulver, S. C.; Fox, B. G.; Solomon, E. I. *J. Am. Chem. Soc.* **1999**, *121*, 2770−2783.
(10) Lindqvist, Y.; Huang, W.; Schneider, G.; Shanklin, J. *EMBO J.* **1996**, *15*, 4081−4092.

10.1021/ic0345976 CCC: $25.00
Published on Web 09/10/2003

Chart 1

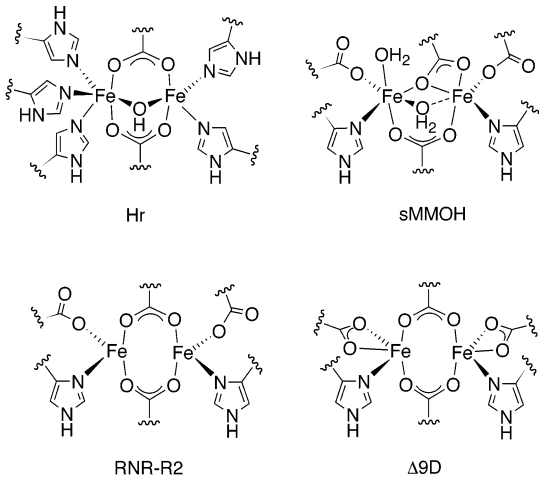

sites of toluene monooxygenase,[3,11] alkene monooxygenase,[12] and phenol hydroxylase.[13] These enzymes effect the oxidation of toluene to cresol, the epoxidation of alkenes, and the conversion of phenol to catechol, respectively.

The remarkable diversity of functions exhibited by these metalloproteins has inspired the synthesis of small molecule model compounds that not only reproduce structural and geometric features of the active sites but also display similar reactivities toward exogenous substrates. A critical incentive for mimicking the chemistry of the enzymes is to understand how modifications in the ligand can affect the steric, electronic, and, ultimately, oxidation properties of complexes in which two iron(II) ions are held in close proximity within a restricted coordination environment. By confining metal centers in a ligand framework that rigorously enforces dinuclearity, the properties of ancillary ligands can be modulated, and these variations can be correlated with the reactivity of the metal compounds.

Diiron complexes have been prepared with bridging carboxylate ligands[1] as well as with a variety of other dinucleating units.[14] The motivation for using non-carboxylate bridging ligands stems from the often unpredictable and undesired formation of high-nuclearity clusters[15−20] or simple monomeric species[1b,21,22] that can occur by self-assembly

Chart 2

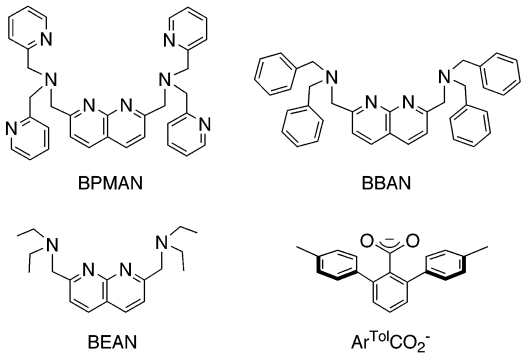

when only carboxylate ligands are employed. One dinucleating spacer that has been applied successfully in our laboratory is 1,8-naphthyridine.[23−28] The similarity in coordination mode of carboxylate and 1,8-naphthyridine for bridging two metal ions suggested to us that it might be considered as a "masked carboxylate." A family of nitrogen-rich, 1,8-naphthyridine-based ligands of varying denticity have been reported[29] and utilized in the synthesis of diiron(II) compounds. In general, these compounds are less reactive toward dioxygen than their carboxylate counterparts, although they have allowed the synthesis of spectroscopic models for oxyHr using H_2O_2.[25]

We report here a series of naphthyridine-based diiron(II) compounds in which the nature of both the multidentate naphthyridine framework and the ancillary bridging ligands are systematically modified. Through these structural variations (Chart 2), the reactivity of the complexes toward dioxygen was altered. The syntheses of the compounds $[Fe_2(BPMAN)(\mu\text{-}O_2CPh)_2](OTf)_2$ (**1**), $[Fe_2(BPMAN)(\mu\text{-}OH)(\mu\text{-}O_2CAr^{Tol})](OTf)_2$ (**2**), $[Fe_2(BPMAN)(\mu\text{-}OMe)(\mu\text{-}O_2CAr^{Tol})](OTf)_2$ (**3**), $[Fe_2(BBAN)(\mu\text{-}O_2CAr^{Tol})_3](OTf)$ (**4**), and $[Fe_2(BEAN)(\mu\text{-}O_2CAr^{Tol})_3](OTf)$ (**5**) are presented.[30] Complexes **1**, **3**, **4**, and **5** were characterized by X-ray crystallography. Cyclic voltammograms of **1**, **2**, and **4** were recorded and the redox potentials were correlated with their observed reactivity toward dioxygen. In addition, the Mössbauer properties of **1**−**4** were investigated. Comparison with related naphthyridine-based diiron systems[23] facilitated a deeper understanding of the influence of the ligand properties on the electrochemical and oxidation chemistry of the complexes.

Experimental Section

General Procedures. Dichloromethane, acetonitrile, diethyl ether, and tetrahydrofuran were saturated with argon and purified

(11) Pikus, J. D.; Studts, J. M.; Achim, C.; Kauffmann, K. E.; Münck, E.; Steffan, R. J.; McClay, K.; Fox, B. G. *Biochemistry* **1996**, *35*, 9106−9119.
(12) Small, F. J.; Ensign, S. A. *J. Biol. Chem.* **1997**, *272*, 24913−24920.
(13) Cadieux, E.; Vrajmasu, V.; Achim, C.; Powlowski, J.; Münck, E. *Biochemistry* **2002**, *41*, 10680−10691.
(14) For a listing of ligands prepared through the functionalization of phenols, pyrazole, naphthyridine, pyridazine, and phthalazine, see references in the following: Kuzelka, J.; Spingler, B.; Lippard, S. J. *Inorg. Chim. Acta* **2002**, *337*, 212−222.
(15) Lee, D.; Sorace, L.; Caneschi, A.; Lippard, S. J. *Inorg. Chem.* **2001**, *40*, 6774−6781.
(16) Mandal, S. K.; Young, V. G., Jr.; Que, L., Jr. *Inorg. Chem.* **2000**, *39*, 1831−1833.
(17) Herold, S.; Lippard, S. J. *Inorg. Chem.* **1997**, *36*, 50−58.
(18) Goldberg, D. P.; Telser, J.; Bastos, C. M.; Lippard, S. J. *Inorg. Chem.* **1995**, *34*, 3011−3024.
(19) Rardin, R. L.; Poganiuch, P.; Bino, A.; Goldberg, D. P.; Tolman, W. B.; Liu, S.; Lippard, S. J. *J. Am. Chem. Soc.* **1992**, *114*, 5240−5249.
(20) Lippard, S. J. *Angew. Chem., Int. Ed. Engl.* **1988**, *27*, 344−361.
(21) Lee, D.; Lippard, S. J. *Inorg. Chim. Acta* **2002**, *341*, 1−11.
(22) Hagadorn, J. R.; Que, L., Jr.; Tolman, W. B. *Inorg. Chem.* **2000**, *39*, 6086−6090.
(23) He, C.; Lippard, S. J. *Inorg. Chem.* **2001**, *40*, 1414−1420.
(24) He, C.; DuBois, J. L.; Hedman, B.; Hodgson, K. O.; Lippard, S. J. *Angew. Chem., Int. Ed.* **2001**, *40*, 1484−1487.
(25) He, C.; Barrios, A. M.; Lee, D.; Kuzelka, J.; Davydov, R. M.; Lippard, S. J. *J. Am. Chem. Soc.* **2000**, *122*, 12683−12690.
(26) He, C.; Gomez, V.; Spingler, B.; Lippard, S. J. *Inorg. Chem.* **2000**, *39*, 4188−4189.
(27) He, C.; Lippard, S. J. *J. Am. Chem. Soc.* **2000**, *122*, 184−185.
(28) He, C.; Lippard, S. J. *Inorg. Chem.* **2000**, *39*, 5225−5231.
(29) He, C.; Lippard, S. J. *Tetrahedron* **2000**, *56*, 8245−8252.
(30) Abbreviations used: OTf^- = triflate; $Ar^{Tol}CO_2^-$ = 2,6-di(*p*-tolyl)-benzoate; BPMAN = 2,7-bis[bis(2-pyridylmethyl)aminomethyl]-1,8-naphthyridine; BBAN = 2,7-bis(*N*,*N*-dibenzylaminomethyl)-1,8-naphthyridine; BEAN = 2,7-bis(*N*,*N*-diethylaminomethyl)-1,8-naphthyridine; $PhCyCO_2^-$ = 1-phenylcyclohexanecarboxylate; Me_3tacn = 1,4,7-trimethyl-1,4,7-triazacyclononane.

by being passed over a column of activated Al_2O_3 under argon.[31] Methanol was distilled from Mg and I_2 under nitrogen. Triethylamine was distilled from CaH_2 under nitrogen. The compounds $Fe(OTf)_2$·2MeCN,[32] BPMAN,[29] BBAN,[29] BEAN,[29] and NaO_2CAr^{Tol} [33−35] were prepared according to published literature procedures. All other reagents were purchased from commercial sources and used as received. Air-sensitive manipulations, including the synthesis of **1**−**5**, were performed by using standard Schlenk techniques or under nitrogen in an MBraun glovebox. Crystalline samples of the diiron(II) complexes were pulverized and heated in vacuo prior to elemental analysis. Removal of the CH_2Cl_2 solvent from solid samples of **1**, **2**, and **4** was incomplete, however, as judged from the analyses.

[Fe$_2$(BPMAN)(μ-O$_2$CPh)$_2$](OTf)$_2$ (1). To a solution of $Fe(OTf)_2$·2MeCN (158 mg, 0.36 mmol) in MeCN (4 mL) was added solid BPMAN (100 mg, 0.18 mmol). The resulting red-orange solution was treated with $PhCO_2H$ (44 mg, 0.36 mmol) and NEt_3 (50 μL, 0.36 mmol) in MeCN (1 mL) to generate a dark red solution that was stirred for 1 h. The solvent was removed under reduced pressure and the residue was dissolved in CH_2Cl_2 and filtered through a plug of Celite. Blue crystals of **1**·CH_2Cl_2, suitable for X-ray diffraction study, were obtained following Et_2O vapor diffusion into this solution (163 mg, 79%). FT-IR (cm^{-1}, KBr): 3431 (w), 3065 (w), 2932 (w), 1608 (s), 1568 (m), 1514 (w), 1480 (w), 1406 (s), 1275 (s), 1262 (s), 1222 (m), 1150(m), 1098 (w), 1070 (w), 1053 (w), 1030 (s), 978 (w), 905 (w), 888 (w), 862 (w), 839 (w), 791 (w), 763 (m), 725 (m), 672 (m), 636 (s), 571 (m), 516 (m). UV−vis (CH_2Cl_2, λ_{max}, nm (ϵ, M^{-1} cm^{-1})) 380 (5800), 600 (1800). Anal. Calcd for **1**·0.25CH_2Cl_2, $Fe_2Cl_{0.5}S_2F_6O_{10}N_8C_{50.25}H_{42.5}$: C, 49.23; H, 3.49; N, 9.14. Found: C, 49.00; H, 3.21; N, 9.46.

[Fe$_2$(BPMAN)(μ-OH)(μ-O$_2$CAr^{Tol})](OTf)$_2$ (2). To a red-orange solution of $Fe(OTf)_2$·2MeCN (158 mg, 0.36 mmol) and BPMAN (100 g, 0.18 mmol) in MeCN (4 mL) was added solid NaO_2CAr^{Tol} (58 mg, 0.18 mmol) to form a brown-green solution. The addition of NEt_3 (25 μL, 0.18 mmol) and argon-saturated H_2O (3.3 μL, 0.18 mmol) resulted in a bright green solution that was stirred for 1 h. Evaporation of the solvent was followed by dissolution of the residue in CH_2Cl_2 and filtration through Celite. Diffusion of Et_2O into this solution yielded **2** as a green flocculent solid (200 mg, 87%). FT-IR (KBr, cm^{-1}): 3509 (w), 3061 (w), 2918 (w), 1603 (m), 1559 (m), 1515 (w), 1480 (w), 1445 (m), 1408 (w), 1382 (w), 1269 (s), 1224 (m), 1155 (m), 1099 (w), 1030 (s), 817 (w), 798 (w), 765 (m), 735 (w), 704 (w), 637 (s), 573 (w), 542 (w), 518 (m). UV−vis (CH_2Cl_2, λ_{max}, nm (ϵ, M^{-1} cm^{-1})) 325 (11 000), 400 (3000), 650 (250). ESI-MS (+*m*/*z*): Calcd for $(M-OTf)^{+1}$ 1131.22, Found 1131.33; Calcd for $\{(M-OTf) + H_2O\}^{+1}$ 1149.23, Found 1149.31; Calcd for $(M-2OTf)^{+2}$ 491.14, Found 491.13; Calcd for $\{(M-2OTf) + H_2O\}^{+2}$ 500.14, Found 500.11. Anal. Calcd for **2**·0.25CH_2Cl_2, $Fe_2Cl_{0.5}S_2F_6O_9N_8C_{57.25}H_{50.5}$: C, 52.81; H, 3.91; N, 8.61. Found: C, 52.59; H, 3.75; N, 8.79.

[Fe$_2$(BPMAN)(μ-OMe)(μ-O$_2$CAr^{Tol})](OTf)$_2$ (3). Vapor diffusion of Et_2O into a solution of **2** (216 mg, 0.17 mmol) in MeOH yielded green blocks of **3**·0.3Et_2O, suitable for X-ray crystallographic analysis (170 mg, 78%). FT-IR (cm^{-1}, KBr): 3503 (w), 3070 (w), 2924 (w), 1605 (m), 1562 (m), 1516 (w), 1480 (w), 1445 (m), 1410 (w), 1384 (w), 1274 (s), 1222 (m), 1153 (m), 1098 (m), 1030 (s), 980 (w), 906 (w), 890 (w), 840 (w), 793 (m), 767 (m), 737 (w), 703 (w), 637 (s), 583 (w), 572 (w), 516 (m). ESI-MS (+*m*/*z*): Calcd for $(M-OTf)^{+1}$ 1145.24, Found 1145.26; Calcd for $(M-2OTf)^{+2}$ 498.14, Found 498.15. Anal. Calcd for **3**, $Fe_2S_2F_6O_9N_8C_{58}H_{52}$: C, 53.80; H, 4.05; N, 8.65. Found: C, 53.90; H, 3.95; N, 8.48.

[Fe$_2$(BBAN)(μ-O$_2$CAr^{Tol})$_3$](OTf) (4). Treatment of $Fe(OTf)_2$·2MeCN (159 mg, 0.36 mmol) with BBAN (100 mg, 0.18 mmol) in MeCN (10 mL) afforded a pale yellow-brown solution. Solid NaO_2CAr^{Tol} (175 mg, 0.54 mmol) was added and the reaction mixture was stirred vigorously for 1 h to generate a pale orange solution. The solvent was evaporated under reduced pressure and the residue was dissolved in CH_2Cl_2 and filtered through Celite. Exposure of this solution to Et_2O vapor diffusion gave tan X-ray quality crystals of **4**·2CH_2Cl_2 (225 mg, 73%). FT-IR (cm^{-1}, KBr): 3057 (m), 3027 (m), 2944 (w), 2920 (m), 2865 (w), 1606 (s), 1587 (s), 1560 (m), 1514 (m), 1496 (w), 1443 (s), 1406 (s), 1386 (s), 1307 (w), 1267 (s), 1222 (m), 1149 (s), 1110 (s), 1071 (w), 1031 (s), 979 (w), 942 (w), 914 (w), 885 (w), 823 (m), 805 (s), 788 (m), 743 (m), 729 (m), 703 (s), 636 (s), 584 (m), 533 (m). Anal. Calcd for **4**·0.5CH_2Cl_2, $Fe_2ClSF_3O_9N_4C_{102.5}H_{88}$: C, 70.11; H, 5.05; N, 3.19. Found: C, 70.09; H, 5.17; N, 3.33.

[Fe$_2$(BEAN)(μ-O$_2$CAr^{Tol})$_3$](OTf) (5). A mixture of $Fe(OTf)_2$·2MeCN (145 mg, 0.33 mmol), BEAN (50 mg, 0.17 mmol), and NaO_2CAr^{Tol} (162 mg, 0.50 mmol) in MeCN (20 mL) was vigorously stirred for 5 h. The suspension was filtered through a medium-porosity frit, and a pale pink solid was collected. The filtrate was evaporated to dryness under reduced pressure, and the resulting solid was dissolved in CH_2Cl_2, filtered through Celite, and exposed to Et_2O vapor diffusion to give tan crystals of **5**·CH_2Cl_2 that were suitable for X-ray diffraction study (44 mg, 18%). The pink solid that was initially collected on the frit was dissolved in MeOH, followed by evaporation of the solvent under reduced pressure. The residue was then dissolved in CH_2Cl_2 and exposed to Et_2O vapor diffusion to give additional **5** (112 mg, 45%). FT-IR (cm^{-1}, KBr): 3054 (w), 3025 (w), 2974 (w), 2936 (w), 2922 (w), 2887 (w), 1609 (m), 1586 (m), 1562 (m), 1514 (m), 1447 (m), 1408 (m), 1385 (s), 1306 (w), 1279 (s), 1261 (s), 1223 (m), 1112 (w), 1084 (w), 1031 (s), 974 (w), 945 (w), 870 (w), 834 (m), 780 (s), 765 (w), 733 (m), 704 (m), 637 (s), 612 (w), 581 (w), 533 (s). Anal. Calcd for **5**, $Fe_2SF_3O_9N_4C_{82}H_{79}$: C, 67.22; H, 5.43; N, 3.82. Found: C, 67.13; H, 5.22; N, 3.98.

Bis(4-methylbenzyl)amine (6). This compound was prepared by an alternative route to published procedures and its properties matched well those reported in the literature.[36−38] A 500-mL round-bottom flask was charged with 4-methylbenzylamine (5 mL, 0.039 mol), tolualdehyde (4.6 mL 0.039 mol), and $NaBH(OAc)_3$ (10.8 g, 0.051 mol) in dichloroethane (200 mL). The reaction mixture was stirred under Ar for 5 h, followed by addition of aqueous NaOH (1 M, 150 mL). The crude product was extracted with CH_2Cl_2 (∼150 mL), dried over $MgSO_4$, and the solvent was removed by rotary evaporation to yield a pale yellow oil. Vacuum distillation afforded a colorless oil with a boiling point of 110−118 °C (0.15 Torr) that was placed under dynamic vacuum overnight to give **6** as a white solid (3.4 g, 39%). ^1H NMR (300 MHz, $CDCl_3$): δ 7.26 m (4H), 7.14 d (J = 26 Hz, 4H), 3.77 s (4H), 2.35 s (6H). FT-IR (cm^{-1}, thin film): 3047 (m), 3019 (m), 2920 (m), 2862 (m), 2819 (m), 1891 (w), 1514 (s), 1450 (m), 1378 (w), 1359 (w), 1303

(31) Pangborn, A. B.; Giardello, M. A.; Grubbs, R. H.; Rosen, R. K.; Timmers, F. J. *Organometallics* **1996**, *15*, 1518−1520.
(32) Hagen, K. S. *Inorg. Chem.* **2000**, *39*, 5867−5869.
(33) Du, C.-J. F.; Hart, H.; Ng, K.-K. D. *J. Org. Chem.* **1986**, *51*, 3162−3165.
(34) Saednya, A.; Hart, H. *Synthesis* **1996**, 1455−1458.
(35) Chen, C.-T.; Siegel, J. S. *J. Am. Chem. Soc.* **1994**, *116*, 5959−5960.
(36) Rao, H. S. P.; Bharathi, B. *Indian J. Chem.* **2002**, *41B*, 1072−1074.
(37) Katritzky, A. R.; Zhao, X.; Hitchings, G. J. *Synthesis* **1991**, 703−708.
(38) Juday, R.; Adkins, H. *J. Am. Chem. Soc.* **1955**, *77*, 4559−4564.

Table 1. Summary of X-ray Crystallographic Information

	1·CH_2Cl_2	**3**·0.3Et_2O	**4**·2CH_2Cl_2	**5**·CH_2Cl_2
formula	$C_{51}H_{42}N_8Fe_2O_{10}S_2F_6Cl_2$	$C_{59.33}H_{52}N_8Fe_2O_{9.33}S_2F_6$	$C_{104}H_{87}N_4Fe_2O_9SF_3Cl_4$	$C_{83}H_{79}N_4Fe_2O_9SF_3Cl_2$
fw	1287.65	1316.24	1879.34	1548.16
space group	*Pccn*	$R\bar{3}$	$P\bar{1}$	*C*2/*c*
a, Å	22.383(3)	29.007(3)	13.525(5)	20.150(3)
b, Å	13.4299(15)		15.559(5)	20.181(3)
c, Å	18.332(2)	37.806(5)	23.417(5)	19.832(3)
α, deg			84.290(5)	
β, deg			89.860(5)	114.242(2)
γ, deg			68.820(5)	
V, Å^3	5510.6(11)	27549(5)	4569(2)	7353.4(18)
Z	4	18	2	4
T, °C	−85	−100	−80	−80
ρ_{calcd}, g cm^{-3}	1.552	1.428	1.366	1.398
μ(Mo Kα), mm^{-1}	0.784	0.623	0.525	0.566
θ range, deg	1.77−25.00	1.35−25.00	1.41−25.00	2.02−28.28
total no. of data	26661	67805	24043	22797
no. of unique data	4848	10788	15910	8431
observed data[a]	3320	8273	10503	6809
no. of parameters	368	782	1164	512
R[b]	0.0627	0.0627	0.0759	0.0632
*w*R2[c]	0.1488	0.1639	0.1964	0.1644
max, min peaks, e Å^{-3}	1.178, −0.587	1.271, −0.310	1.064, −1.184	0.613, −0.960

[a] Observation criterion: $I > 2\sigma(I)$. [b] $R = \sum||F_o| - |F_c||/\sum|F_o|$. [c] $wR^2 = \{\sum[w(F_o^2 - F_c^2)^2]/\sum[w(F_o^2)^2]\}^{1/2}$.

(w), 1198 (w), 1177 (w), 1101 (m), 1040 (w), 1021 (w), 845 (w), 806 (s), 772 (m), 719 (w), 695 (w), 584 (m), 486 (m).

Procedures for Amine *N*-Dealkylation Studies. Samples were prepared and analyzed following a procedure described elsewhere.[39] For the oxidation of bis(4-methylbenzyl)amine, 2 equiv (with respect to the diiron(II) compound) were added to a solution of **4** or **5** prior to addition of the oxidant.

Physical Measurements. ^{1}H NMR spectra were obtained on a 300 MHz Varian Unity spectrometer. FT-IR spectra were measured on a Thermo Nicolet Avatar 360 spectrometer. Optical spectra were collected on a Hewlett-Packard 8453 diode-array spectrophotometer; experiments were performed by using a custom-made quartz cuvette fused onto a vacuum-jacketed Dewar. EPR spectra of reaction mixtures of **2** with dioxygen were recorded as frozen solutions on a Bruker model 300 ESP X-Band spectrometer (9.37 GHz) running WinEPR software. A specially designed coldfinger with liquid N_2 was used to maintain the temperature at 77 K. ESI-MS spectra of **2** and **3** were obtained as solutions in MeCN on a Bruker Daltonics APEXII 3 T Fourier Transform Mass Spectrometer in the MIT Department of Chemistry Instrumentation Facility.

X-ray Crystallography. Crystals were mounted in Paratone N oil on the ends of glass capillaries and frozen into place under a low-temperature nitrogen cold stream. Data were collected on a Bruker (formerly Siemens) SMART (**1**, **4**, **5**) or APEX (**3**) CCD X-ray diffractometer running the SMART software package,[40] with Mo Kα radiation (λ = 0.71073 Å), and refined using SAINT software.[41] Details of the data collection and reduction protocols are described elsewhere.[42] The structures were solved by direct methods using SHELXS-97 software[43] and refined on F^2 by using the SHELXL-97 program[44] incorporated in the SHELXTL software package.[45] Empirical absorption corrections were applied with SADABS,[46] and the possibility of higher symmetry was checked by the program PLATON.[47] All non-hydrogen atoms were located, and their positions were refined with anisotropic thermal parameters by least-squares cycles and Fourier syntheses. Hydrogen atoms were assigned idealized positions and given a thermal parameter 1.2 times that of the carbon atom to which each was attached.

The structure of **3** contains one ordered and one disordered triflate counterion. The three positions of the disordered triflate moiety are located on an inversion center, a 3-fold axis, and an inversion center combined with a 3-fold axis, respectively. They are all fully occupied, but because of the symmetry, only contribute 50, 33, and 17% to the content of the asymmetric unit. Two of the partially occupied triflate units contained positionally disordered SO_3 and CF_3 moieties. A diethyl ether solvent molecule was refined with 33% occupancy. Additional high residual electron density (1.27 e Å^{-3}) located on a special position near a triflate counterion was not modeled. The structure of **4** contains a CH_2Cl_2 solvent molecule, the carbon and one chlorine atom of which were disordered and modeled over two positions, each with 50% occupancy. The carbon atom of the CH_2Cl_2 solvent molecule in structure **5** was disordered over two positions, each refined with occupancies of 50%. In addition, two half-occupied triflate counterions were present in the lattice, the SO_3 and CF_3 components of which were positionally disordered. Crystallographic information for compounds **1**, **3**, **4**, and **5** is provided in Table 1, and Figures S4− S7 in the Supporting Information show the structures with complete atom-labeling schemes.

Electrochemistry. Cyclic voltammograms were recorded in an MBraun glovebox under a nitrogen atmosphere using an EG&G model 263 potentiostat. The cell contained a platinum working electrode, a $Ag/AgNO_3$ (0.1 M in MeCN) reference electrode, and a platinum wire auxiliary electrode. A 0.5 M $Bu_4N(PF_6)$ solution was used as the supporting electrolyte. All measurements were

(39) Lee, D.; Lippard, S. J. *Inorg. Chem.* **2002**, *41*, 827−837.
(40) *SMART v5.626: Software for the CCD Detector System*; Bruker AXS: Madison, WI, 2000.
(41) *SAINT v5.01: Software for the CCD Detector System*; Bruker AXS: Madison, WI, 1998.
(42) Feig, A. L.; Bautista, M. T.; Lippard, S. J. *Inorg. Chem.* **1996**, *35*, 6892−6898.
(43) Sheldrick, G. M. *SHELXS-97: Program for the Solution of Crystal Structure*; University of Göttingen: Göttingen, Germany, 1997.
(44) Sheldrick, G. M. *SHELXL-97: Program for the Solution of Crystal Structure*; University of Göttingen: Göttingen, Germany, 1997.
(45) *SHELXTL v5.10: Program Library for Structure Solution and Molecular Graphics*; Bruker AXS: Madison, WI, 1998.
(46) Sheldrick, G. M. *SADABS: Area-Detector Absorption Correction*; University of Göttingen: Göttingen, Germany, 1996.
(47) Spek, A. L. *PLATON, A Multipurpose Crystallographic Tool*; Utrecht University: Utrecht, The Netherlands, 2000.

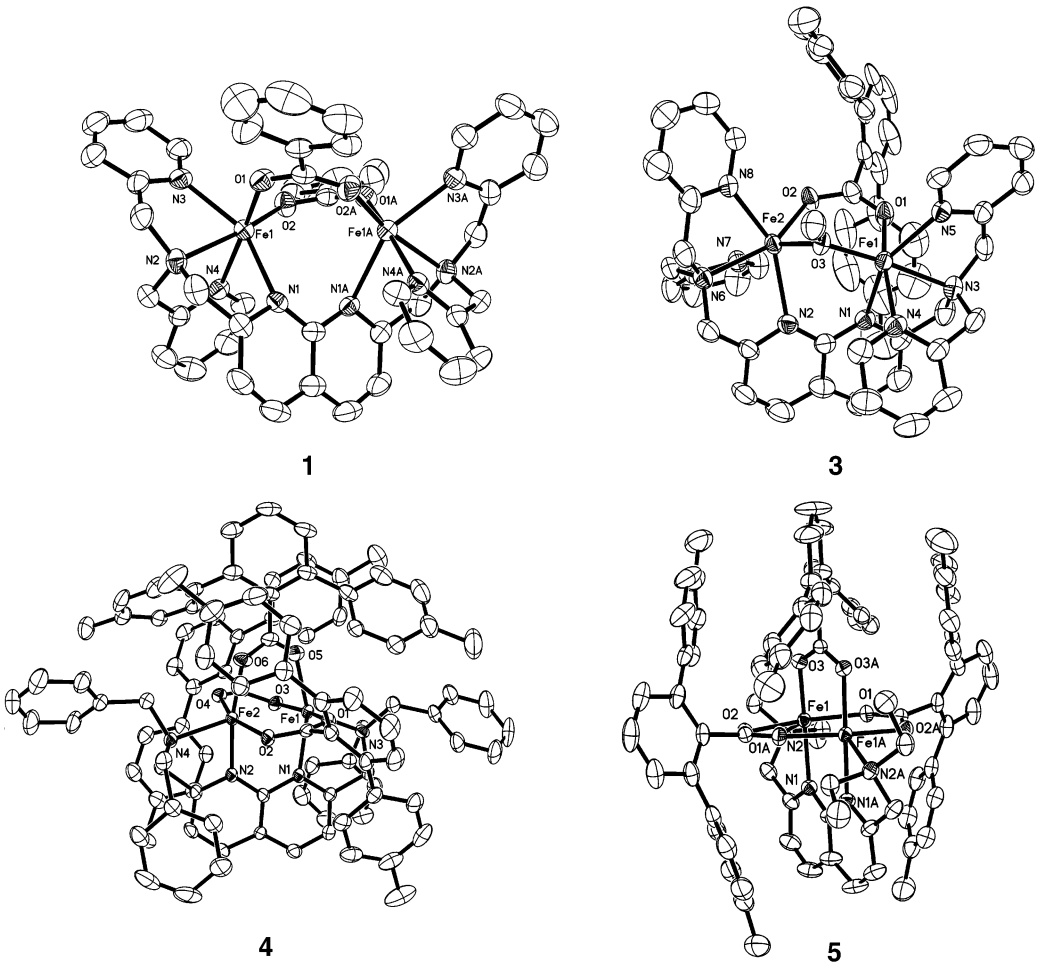

Figure 1. ORTEP diagrams of the cations of $[Fe_2(BPMAN)(\mu\text{-}O_2CPh)_2](OTf)_2$ (**1**), $[Fe_2(BPMAN)(\mu\text{-}OMe)(\mu\text{-}O_2CAr^{Tol})](OTf)_2$ (**3**), $[Fe_2(BBAN)(\mu\text{-}O_2CAr^{Tol})_3](OTf)$ (**4**), and $[Fe_2(BEAN)(\mu\text{-}O_2CAr^{Tol})_3](OTf)$ (**5**) showing 50% probability thermal ellipsoids for all non-hydrogen atoms.

externally referenced to ferrocene. Plots of current vs (scan rate)$^{1/2}$ for **1** and **2** are linear, as displayed in Figures S1 and S2 in the Supporting Information.

Mössbauer Spectroscopy. Mössbauer spectra (4.2 K) were recorded in the MIT Department of Chemistry Instrumentation Facility on an MS1 spectrometer (WEB Research Co.) with a ^{57}Co source in a Rh matrix kept at room temperature. Spectra were fit to Lorentzian line shapes by using the WMOSS plot and fit program,[48] and isomer shifts were referenced to natural abundance Fe at room temperature. Solid samples were prepared by suspending powdered material (~0.04 mmol) in Apiezon N grease and placing the mixture in a nylon sample holder. Frozen solutions (~50 mM) were prepared by transferring ~800 μL of a solution generated in a septum-sealed vial to a nylon sample holder via a gastight syringe. The solutions were then flash-frozen in liquid N_2.

Results

Synthesis and Structural Characterization of the Bis(carboxylato)diiron(II) Complex $[Fe_2(BPMAN)(\mu\text{-}O_2CPh)_2](OTf)_2$ (1). The reaction of $Fe(OTf)_2$·2MeCN with BPMAN, $PhCO_2H$, and NEt_3 in a 2:1:2:2 ratio afforded compound **1** as a blue solid in good yield (79%). Figure 1 shows the structure of **1**, and Table 2 lists selected bond lengths and angles. The crystallographically equivalent iron centers have distorted octahedral stereochemistry and are bridged by the naphthyridine moiety of BPMAN, as well as by the two

Table 2. Selected Bond Lengths (Å) and Angles (deg) for **1**·CH_2Cl_2 and **3**·0.3Et_2O[a]

bond lengths		bond angles	
		1·CH_2Cl_2	
Fe(1)···Fe(1A)	3.790(2)	N(4)−Fe(1)−O(1)	166.14(15)
Fe(1)−N(1)	2.334(4)	N(3)−Fe(1)−N(1)	149.66(15)
Fe(1)−N(2)	2.231(4)	N(3)−Fe(1)−O(2)	93.76(15)
Fe(1)−N(3)	2.212(4)	N(2)−Fe(1)−N(1)	75.08(14)
Fe(1)−N(4)	2.180(4)	N(2)−Fe(1)−O(2)	162.54(14)
Fe(1)−O(1)	2.088(3)	N(1)−Fe(1)−O(2)	115.98(14)
Fe(1)−O(2)	1.994(3)	N(2)−Fe(1)−O(1)	89.33(14)
		3·0.3Et_2O	
Fe(1)···Fe(2)	3.237(1)	Fe(1)−O(3)−Fe(2)	108.48(12)
Fe(1)−N(1)	2.296(3)	O(1)−Fe(1)−O(3)	99.26(11)
Fe(1)−N(3)	2.233(3)	O(2)−Fe(2)−O(3)	95.17(10)
Fe(1)−N(4)	2.188(3)	N(3)−Fe(1)−O(3)	173.17(12)
Fe(1)−N(5)	2.257(3)	N(4)−Fe(1)−O(3)	94.36(12)
Fe(1)−O(1)	2.123(3)	N(5)−Fe(1)−O(3)	107.05(12)
Fe(1)−O(3)	1.959(2)	N(1)−Fe(1)−O(1)	89.88(12)
Fe(2)−N(2)	2.328(3)	N(4)−Fe(1)−O(1)	164.89(12)
Fe(2)−N(6)	2.260(3)	N(6)−Fe(2)−O(3)	111.61(11)
Fe(2)−N(7)	2.250(3)	N(7)−Fe(2)−O(3)	162.85(11)
Fe(2)−N(8)	2.207(3)	N(8)−Fe(2)−O(3)	93.92(11)
Fe(2)−O(2)	2.083(3)	N(2)−Fe(2)−O(2)	120.08(12)
Fe(2)−O(3)	2.030(3)	N(6)−Fe(2)−O(2)	150.27(11)

[a] Numbers in parentheses are estimated standard deviations of the last significant figure. Atoms are labeled as indicated in Figure 1.

(48) Kent, T. A. *WMoss v2.5: Mössbauer Spectral Analysis Software*; WEB Research Co.: Minneapolis, MN, 1998.

benzoate ligands (Fe···Fe = 3.790(2) Å). The Fe−N(naphthyridine) bond length of 2.334(4) Å is substantially longer than the corresponding pyridine and amine distances, which average 2.208(2) Å. The carboxylate groups are coordinated to the iron(II) centers with Fe−O distances of 2.088(3) and 1.994(3) Å, with the shorter bond disposed trans to the amine nitrogen atom of BPMAN. The geometric parameters of **1** are similar to that of the related complex $[Fe_2(BPMAN)(\mu\text{-}O_2CPhCy)_2](OTf)_2$ prepared previously in our laboratory.[23]

Synthesis and Characterization of the Hydroxide- and Methoxide-Bridged Compounds $[Fe_2(BPMAN)(\mu\text{-}OH)(\mu\text{-}O_2CAr^{Tol})](OTf)_2$ (2) and $[Fe_2(BPMAN)(\mu\text{-}OMe)(\mu\text{-}O_2CAr^{Tol})](OTf)_2$ (3). Compound **2** was prepared as a green flocculent solid in high yield (87%) by allowing 2 equiv of $Fe(OTf)_2 \cdot 2MeCN$ to react with 1 equiv each of BPMAN, NaO_2CAr^{Tol}, H_2O, and NEt_3. X-ray quality crystals of **2** could not be obtained despite numerous attempts, but ESI-MS confirmed its identity. Two sets of signals that correspond to monocations were detected. These were identified as the parent compound, minus a triflate anion, in the presence (m/z = 1149.31) or absence (m/z = 1131.33) of a molecule of water. Signals belonging to dications were also identified and assigned to the parent compound following loss of both triflate counterions ($(M - 2OTf)^{+2}$, 491.13; $\{(M - 2OTf) + H_2O\}^{+2}$, 500.11). The water was most likely introduced from the MeCN solvent in which this measurement was performed. All four experimental values match well with the calculated masses.

Recrystallization of **2** from a solution of MeOH and Et_2O afforded the methoxide derivative, compound **3**, in 78% yield. As with the hydroxide derivative, **3** was analyzed by ESI-MS and signals corresponding to both the monocation (m/z = 1145.26) and dication (m/z = 498.15) were observed. Fortunately, X-ray quality crystals of **3** were obtained, permitting a full structural analysis. Figure 1 shows the structure and Table 2 lists selected bond lengths and angles. The two iron centers are triply bridged by the naphthyridine unit of BPMAN and the carboxylate and methoxide ligands. The metal−metal separation of 3.237(1) Å is contracted relative to that of **1** ($\Delta_{Fe\cdots Fe}$ = 0.553(2) Å), reflecting the presence of the single atom bridge in **3**. The methoxide unit is coordinated to the distorted octahedral iron(II) centers with Fe−O bond lengths of 1.959(2) and 2.030(3) Å, and the Fe−O−Fe bond angle is 108.48(12)°. The Fe−O distances of the bound $Ar^{Tol}CO_2^-$ ligand are 2.123(3) and 2.083(3) Å, and the Fe−N bonds average 2.252(1) Å. The significant steric bulk of the carboxylate moiety forces the terphenyl group to lie approximately perpendicular to the Fe···Fe vector in order to avoid interaction with the pyridine groups of the BPMAN ligand. Attempts to prepare the bis(μ-carboxylato) complex were unsuccessful, but an examination of the structure of **3** reveals that such a compound is unlikely to form because of the resulting steric interactions. The position of the carboxylate ligand leaves the opposite face on which the methoxide unit is located largely exposed. The structural features of **3** closely resemble those of $[Fe_2(BPMAN)(\mu\text{-}OH)(\mu\text{-}O_2CPhCy)](OTf)_2$,[23] and a similar coordination environment is expected for the hydroxide-bridged complex **2**.

Whereas numerous methoxide-bridged diiron(III) compounds are known,[49−54] a survey of the Cambridge Structural Database revealed that no dinuclear iron(II) complexes with bridging methoxide ligands have been crystallographically characterized. The (μ_3−OMe)triiron unit is frequently encountered as a component of iron(II) alkoxide cubes[55,56] and in mixed-valent dodecairon oxo compounds, however.[57−59] The octadentate BPMAN ligand and the sterically hindered $Ar^{Tol}CO_2^-$ moieties of **3** stabilize the coordination of methoxide as a ligand bridge between only two metal ions, preventing the formation of higher nuclearity species.

Preparation and Crystallographic Analysis of the Paddle-Wheel Compounds $[Fe_2(BBAN)(\mu\text{-}O_2CAr^{Tol})_3](OTf)$ (4) and $[Fe_2(BEAN)(\mu\text{-}O_2CAr^{Tol})_3](OTf)$ (5). The synthesis of complex **4** was achieved by allowing 2 equiv of $Fe(OTf)_2 \cdot 2MeCN$ to react with BBAN and NaO_2CAr^{Tol} in a 1:3 ratio. Tan crystals of **4** were obtained in good yield (73%) upon recrystallization from CH_2Cl_2/Et_2O. The structure of **4** is shown in Figure 1, and selected bond lengths and angles are provided in Table 3. In addition to the naphthyridine unit of BBAN, the pseudo square-pyramidal iron centers are bridged by three carboxylate ligands. The quadruply-bridged core results in a short Fe···Fe separation of 2.854(2) Å, similar to the inter-metal distances of tetrakis(μ-carboxylato)diiron(II) complexes.[60−62] The Fe−N bond lengths in **4** are demonstrably shorter ($Fe-N_{av}$ = 2.181(2) Å) than the corresponding bonds in **1** and **3** (Δ_{Fe-N} = 0.102(4) and 0.0980(3) Å, respectively), reflecting the lower coordination number of the iron centers in **4**. The Fe−O bond lengths range from 2.035(3) to 2.110(3) Å with one metal site, Fe(2), having a particularly long Fe−O bond (Fe(2)−O(4) = 2.110(3) Å) and an unusually short Fe−N bond

(49) Westerheide, L.; Müller, F. K.; Than, R.; Krebs, B.; Dietrich, J.; Schindler, S. *Inorg. Chem.* **2001**, *40*, 1951−1961.
(50) Scarpellini, M.; Neves, A.; Bortoluzzi, A. J.; Vencato, I.; Drago, V.; Ortiz, W. A.; Zucco, C. *J. Chem. Soc., Dalton Trans.* **2001**, 2616−2623.
(51) Viswanathan, R.; Palaniandavar, M.; Prabakaran, P.; Muthiah, P. T. *Inorg. Chem.* **1998**, *37*, 3881−3884.
(52) Le Gall, F.; de Biani, F. F.; Caneschi, A.; Cinelli, P.; Cornia, A.; Fabretti, A. C.; Gatteschi, D. *Inorg. Chim. Acta* **1997**, *262*, 123−132.
(53) Barclay, S. J.; Riley, P. E.; Raymond, K. N. *Inorg. Chem.* **1984**, *23*, 2005−2010.
(54) Chiari, B.; Piovesana, O.; Tarantelli, T.; Zanazzi, P. F. *Inorg. Chem.* **1982**, *21*, 1396−1402.
(55) Clemente-Juan, J. M.; Mackiewicz, C.; Verelst, M.; Dahan, F.; Bousseksou, A.; Sanakis, Y.; Tuchagues, J.-P. *Inorg. Chem.* **2002**, *41*, 1478−1491.
(56) Taft, K. L.; Caneschi, A.; Pence, L. E.; Delfs, C. D.; Papaefthymiou, G. C.; Lippard, S. J. *J. Am. Chem. Soc.* **1993**, *115*, 11753−11766.
(57) Caneschi, A.; Cornia, A.; Lippard, S. J.; Papaefthymiou, G. C.; Sessoli, R. *Inorg. Chim. Acta* **1996**, *243*, 295−304.
(58) Taft, K. L.; Papaefthymiou, G. C.; Lippard, S. J. *Inorg. Chem.* **1994**, *33*, 1510−1520.
(59) Taft, K. L.; Papaefthymiou, G. C.; Lippard, S. J. *Science* **1993**, *259*, 1302−1305.
(60) Lee, D.; Lippard, S. J. *Inorg. Chem.* **2002**, *41*, 2704−2719.
(61) Chavez, F. A.; Ho, R. Y. N.; Pink, M.; Young, V. G., Jr.; Kryatov, S. V.; Rybak-Akimova, E. V.; Andres, H.; Münck, E.; Que, L., Jr.; Tolman, W. B. *Angew. Chem., Int. Ed.* **2002**, *41*, 149−152.
(62) Randall, C. R.; Shu, L.; Chiou, Y.-M.; Hagen, K. S.; Ito, M.; Kitajima, N.; Lachicotte, R. J.; Zang, Y.; Que, L., Jr. *Inorg. Chem.* **1995**, *34*, 1036−1039.

Table 3. Selected Bond Lengths (Å) and Angles (deg) for **4**·$2CH_2Cl_2$ and **5**·CH_2Cl_2[a]

bond lengths		bond angles	
		4·$2CH_2Cl_2$	
Fe(1)·· ·Fe(2)	2.854(2)	N(1)−Fe(1)−O(1)	87.73(13)
Fe(1)−N(1)	2.205(4)	N(1)−Fe(1)−O(3)	91.01(13)
Fe(1)−N(3)	2.197(4)	O(1)−Fe(1)−O(5)	88.83(13)
Fe(1)−O(1)	2.072(3)	N(3)−Fe(1)−O(1)	93.59(13)
Fe(1)−O(3)	2.035(3)	N(3)−Fe(1)−O(5)	124.36(14)
Fe(1)−O(5)	2.066(3)	N(3)−Fe(1)−O(3)	100.81(14)
Fe(2)−N(2)	2.138(4)	N(2)−Fe(2)−O(2)	95.28(13)
Fe(2)−N(4)	2.182(4)	N(2)−Fe(2)−O(4)	85.89(13)
Fe(2)−O(2)	2.068(3)	O(2)−Fe(2)−O(6)	87.59(13)
Fe(2)−O(4)	2.110(3)	O(4)−Fe(2)−O(6)	86.51(12)
Fe(2)−O(6)	2.038(3)	N(4)−Fe(2)−O(4)	97.27(13)
		5·CH_2Cl_2	
Fe(1)···Fe(1A)	2.890(1)	N(1)−Fe(1)−O(1)	91.72(10)
Fe(1)−N(1)	2.207(3)	N(1)−Fe(1)−O(2)	84.46(10)
Fe(1)−N(2)	2.170(3)	O(1)−Fe(1)−O(3)	90.17(9)
Fe(1)−O(1)	2.045(2)	O(2)−Fe(1)−O(3)	87.31(9)
Fe(1)−O(2)	2.089(2)	N(2)−Fe(1)−O(1)	104.33(10)
Fe(1)−O(3)	2.048(2)	N(2)−Fe(1)−O(3)	119.98(10)

[a] Numbers in parentheses are estimated standard deviations of the last significant figure. Atoms are labeled as indicated in Figure 1.

length (Fe(2)−N(2) = 2.138(4) Å). Because the 1,8-naphthyridine moiety can be thought of as a masked carboxylate, the structure of **4** is best described as a paddle-wheel, with four approximately orthogonal adjacent "carboxylate" groups.

Complex **5** was prepared by following a similar procedure, except that the ligand BEAN bearing dangling ethyl groups was used in place of the benzyl derivative BBAN. The resulting tan crystalline solid was initially isolated in low yield (18%) due to the precipitation of a pink material over the course of the reaction. Although not soluble in MeCN, CH_2Cl_2, or THF, this solid could be dissolved in MeOH and single crystals were grown from a solution of MeOH and Et_2O. An X-ray diffraction study of these crystals revealed the structure of **5**. Presumably, the pink solid that initially forms is a polymeric material that converts into discrete dinuclear units in MeOH. Therefore, recrystallization of this solid increases the isolated yield of **5** to 63%.

Figure 1 shows the structure of **5**, and pertinent bond lengths and angles are listed in Table 3. The square-pyramidal iron(II) centers are separated by 2.890(1) Å, and the average Fe−N and Fe−O bond lengths of this paddle-wheel complex are 2.189(2) and 2.061(1) Å, respectively. The structural parameters of **4** and **5** are similar, and match well with those of the related compound [Fe_2(BEAN)(μ-O_2CPhCy)$_3$](OTf).[23]

Mössbauer Spectroscopic Properties of Diiron(II) Compounds. Zero-field Mössbauer spectra of powdered samples of **1**−**4** were recorded at 4.2 K. Spectra are displayed in Figure 2, and extracted parameters are provided in Table 4. The isomer shifts and quadrupole splittings are typical of high-spin iron(II) compounds in an N/O coordination environment.[63−65] The extracted Mössbauer parameters of the four compounds closely resemble those of related complexes.[23] Noteworthy is the spectrum of **4**, in which the

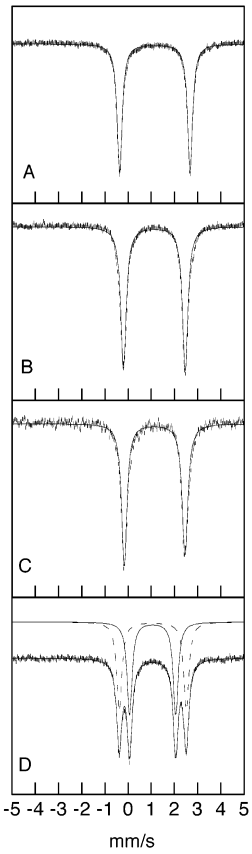

Figure 2. Mössbauer spectra (experimental data (|), calculated fit (−)) recorded at 4.2 K for solid samples of [Fe_2(BPMAN)(μ-O_2CPh)$_2$](OTf)$_2$ (**1**) (A); [Fe_2(BPMAN)(μ-OH)(μ-O_2CAr^{Tol})](OTf)$_2$ (**2**) (B); [Fe_2(BPMAN)-(μ-OMe)(μ-O_2CAr^{Tol})](OTf)$_2$ (**3**) (C); [Fe_2(BBAN)(μ-O_2CAr^{Tol})$_3$](OTf) (**4**) (D). The upper curves of D show two subsets for the calculated spectrum.

Table 4. Summary of Mössbauer Parameters for Compounds **1**−**4** Recorded at 4.2 K (mm s^{-1})

complex	δ	ΔE_Q	Γ
1	1.16(2)	3.03(2)	0.25
2	1.13(2)	2.66(2)	0.28
3	1.14(2)	2.62(2)	0.27 (Γ_L)
			0.29 (Γ_R)
4	1.06(2)	1.99(2)	0.26
	1.06(2)	2.89(2)	0.27

two quadrupole doublets are well resolved. The doublets were fit with identical isomer shifts and significantly different quadrupole splitting values, $\Delta(\Delta E_Q)$ = 0.9 mm s^{-1}. This model was chosen over one in which the two doublets have similar quadrupole splitting parameters (δ_1 = 1.29(2), ΔE_{Q1} = 2.45(2), δ_2 = 0.84(2), ΔE_{Q2} = 2.44(2) mm s^{-1}) because of the unusually low value of δ_2 required to fit the data. Two well-defined doublets were similarly observed in the Mössbauer spectrum of [Fe_2(BEAN)(μ-O_2CPhCy)$_3$](OTf).[23] Both **4** and [Fe_2(BEAN)(μ-O_2CPhCy)$_3$](OTf) contain one iron site, Fe(2) in **4**, that is in a more asymmetric environment than the other. As suggested for [Fe_2(BEAN)(μ-O_2CPhCy)$_3$]-(OTf), the crystallographically observed asymmetry of the

(63) Kurtz, D. M., Jr. *Chem. Rev.* **1990**, *90*, 585−606.

(64) Gütlich, P.; Ensling, J. In *Inorganic Electronic Structure and Spectroscopy*; Solomon, E. I., Lever, A. B. P., Eds.; John Wiley & Sons: New York, 1999; Vol. I, pp 161−211.

(65) Münck, E. In *Physical Methods in Bioinorganic Chemistry: Spectroscopy and Magnetism*; Que, L., Jr., Ed.; University Science Books: Sausalito, CA, 2000; pp 287−319.

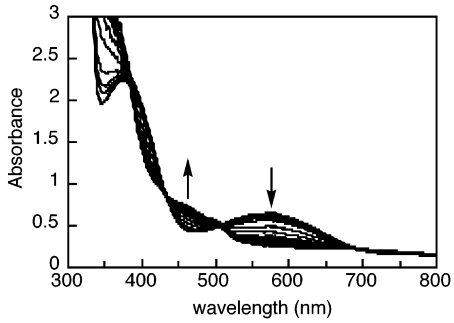

Figure 3. UV-vis spectra accompanying the reaction of $[Fe_2(BPMAN)(\mu\text{-}O_2CPh)_2](OTf)_2$ (**1**) with 5 equiv 30% aqueous H_2O_2, 0.4 mM in MeCN at −40 °C.

iron centers in **4** may give rise to the large difference in quadrupole splitting parameters.

Reactions of 1 with Dioxygen and H_2O_2. The reaction between **1** and dioxygen was monitored by UV−visible spectroscopy. A solution of **1** in CH_2Cl_2 is blue, and we assigned the optical band ($\lambda_{max} = 600$ nm; $\epsilon \approx 1800$ M^{-1} cm^{-1}) as a metal-to-ligand charge transfer (MLCT) transition.[66] Compound **1** is unreactive toward dioxygen at −78 °C, but at room temperature two new features appear at 450 nm ($\epsilon \approx 1700$ M^{-1} cm^{-1}) and 500 nm ($\epsilon \approx 1500$ M^{-1} cm^{-1}) over a period of 2 h. Similar behavior was observed when the oxygenation was carried out in MeCN. As shown in Figure 3, treatment of **1** with H_2O_2 in MeCN at −40 °C resulted in clean conversion to a similar species with shoulders at 450 nm ($\epsilon \approx 1900$ M^{-1} cm^{-1}) and 500 nm ($\epsilon \approx 1500$ M^{-1} cm^{-1}). These spectral features are consistent with the formation of a (μ-oxo)diiron(III) complex.[63,67−70] The frozen solution Mössbauer spectrum of **1** following treatment with H_2O_2 in MeCN revealed a new species that was fit as a quadrupole doublet with $\delta = 0.47(2)$ and $\Delta E_Q = 1.59(2)$ mm s^{-1} (Figure S3A in the Supporting Information). These parameters are typical for high-spin iron(III) centers and resemble those of (μ-oxo)(μ-carboxylato)$_n$diiron(III) ($n = 1$ or 2) cores supported in nitrogen-rich ligand frameworks.[67,71,72] Because both iron centers of **1** are six-coordinate, the introduction of a bridging oxo ligand would probably be accompanied by a carboxylate shift[73] to make available the requisite O-binding sites, as has been suggested for both diiron model compounds and protein cores.[68,74−76]

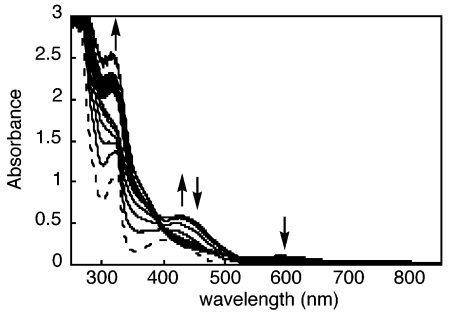

Figure 4. UV-vis spectra accompanying the reaction of $[Fe_2(BPMAN)(\mu\text{-}OH)(\mu\text{-}O_2CAr^{Tol})](OTf)_2$ (**2**) with excess O_2, 0.1 mM in CH_2Cl_2 at room temperature.

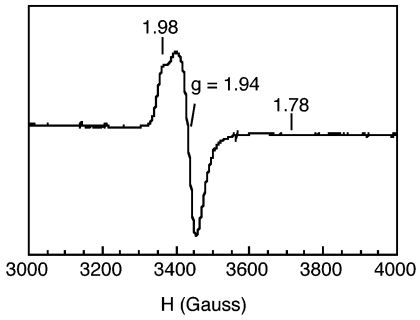

Figure 5. X-band EPR spectrum of $[Fe_2(BPMAN)(\mu\text{-}OH)(\mu\text{-}O_2CAr^{Tol})](OTf)_2$ (**2**) exposed to O_2 as a frozen solution (5 mM in CH_2Cl_2) at 77 K.

Formation of Fe(II)Fe(III) Species from Compounds 2 and 3. Upon exposure to dioxygen, a green solution of **2** in CH_2Cl_2 gradually turns brown. Within ∼20 min, a new band, shown in Figure 4, at 430 nm ($\epsilon \approx 6000$ M^{-1} cm^{-1}) forms, and decay of this same band begins within 1 h. The final product has shoulders at 450 and 500 nm ($\epsilon \approx 2000$ and 1500 M^{-1} cm^{-1}, respectively). Similar behavior was observed with the methoxide derivative **3**. The spectral features of the oxidation product of **2** resemble those resulting from the oxidation of **1**, and suggest that the final species is a (μ-oxo)diiron(III) complex. The Mössbauer spectrum of this compound ($\delta = 0.46(2)$ and $\Delta E_Q = 1.71(2)$ mm s^{-1}, Figure S3B in the Supporting Information) is consistent with high-spin Fe(III) centers and the large quadrupole splitting value is characteristic of a bridging oxo ligand.

To investigate the nature of the intermediate ($\lambda_{max} = 430$ nm), EPR spectroscopy was employed. At 77 K, the diiron(II) compound is EPR silent. A signal was observed, however, one minute after oxygenation of the solution. Figure 5 displays the resulting rhombic spectrum with $g_x = 1.98$, $g_y = 1.94$, and $g_z = 1.78$, typical of antiferromagnetically coupled high-spin Fe(II)Fe(III) ions having an $S = 1/2$ ground state.[77] The $S = 1/2$ signal accounts for up to 20% of the total iron content in the sample, consistent with UV−visible spectroscopic studies that reveal the intermediate to decompose more rapidly at the concentrations used for the EPR measurements (1−5 mM), and with the Mössbauer

(66) Baik, M.; Kuzelka, J.; Lippard, S. J.; Friesner, R. A. Unpublished results. Transition dipole moment calculations on **2** indicate that the HOMO−LUMO electronic transition probability, $|\mu|^2$, is 0.056 D^2. This corresponds to a metal-to-ligand charge-transfer excitation.
(67) Tshuva, E. Y.; Lee, D.; Bu, W.; Lippard, S. J. *J. Am. Chem. Soc.* **2002**, *124*, 2416−2417.
(68) White, M. C.; Doyle, A. G.; Jacobsen, E. N. *J. Am. Chem. Soc.* **2001**, *123*, 7194−7195.
(69) Ménage, S.; Que, L., Jr. *New J. Chem.* **1991**, *15*, 431−438.
(70) Norman, R. E.; Yan, S.; Que, L., Jr.; Backes, G.; Ling, J.; Sanders-Loehr, J.; Zhang, J. H.; O'Connor, C. J. *J. Am. Chem. Soc.* **1990**, *112*, 1554−1562.
(71) Yan, S.; Cox, D. D.; Pearce, L. L.; Juarez-Garcia, C.; Que, L., Jr.; Zhang, J. H.; O'Connor, C. J. *Inorg. Chem.* **1989**, *28*, 2509−2511.
(72) Hartman, J. R.; Rardin, R. L.; Chaudhuri, P.; Pohl, K.; Wieghardt, K.; Nuber, B.; Weiss, J.; Papaefthymiou, G. C.; Frankel, R. B.; Lippard, S. J. *J. Am. Chem. Soc.* **1987**, *109*, 7387−7396.
(73) Rardin, R. L.; Tolman, W. B.; Lippard, S. J. *New. J. Chem.* **1991**, *15*, 417−430.
(74) Whittington, D. A.; Lippard, S. J. *J. Am. Chem. Soc.* **2001**, *123*, 827−838.
(75) Högbom, M.; Andersson, M. E.; Nordlund, P. *J. Biol. Inorg. Chem.* **2001**, *6*, 315−323.
(76) Torrent, M.; Musaev, D. G.; Morokuma, K. *J. Phys. Chem. B* **2001**, *105*, 322−327.
(77) Bertrand, P.; Guigliarelli, B.; More, C. *New. J. Chem.* **1991**, *15*, 445−454.

spectrum of the final oxidized product showing ~50% of unreacted **2**. A much weaker signal at $g \approx 4$ (not shown) may arise from a mononuclear impurity. Spectra recorded at later time points (5−195 min after oxygenation) are more isotropic and less intense. The EPR spectrum of the intermediate matches well those of (μ-oxo)diiron(II,III) centers prepared by chemical,[78] electrochemical,[79] and radiolytic methods,[80−82] and is distinct from those of (μ-hydroxo)diiron(II,III) systems.[81−83]

We interpret these spectroscopic features to arise from the formation of a mixed-valent, oxo-bridged Fe(II)Fe(III) intermediate that decomposes to a (μ-oxo)diiron(III) species. A similar reaction was observed in the oxidation of a series of (μ-hydroxo)diiron(II) complexes supported by Me_3tacn ligands in MeCN and was attributed to outer-sphere electron transfer.[30,78] In contrast, the mixed-valent intermediate is not observed when the oxidation of **2** is performed in MeCN, possibly because the reaction of **2** with dioxygen occurs by an inner-sphere mechanism, in which a carboxylate shift is necessary to open a site for dioxygen coordination. Use of a coordinating solvent such as MeCN may prevent direct interaction between the iron(II) center and dioxygen. Mixed-valent diiron(II,III) species also result from the reaction between dioxygen and the carboxylate-rich compounds, $[Fe_2(\mu\text{-}O_2CAr^{Tol})_2(O_2CAr^{Tol})_2(C_5H_5N)_2]$ and $[Fe_2(\mu\text{-}O_2CAr^{Tol})_4(4\text{-}^tBuC_5H_4N)_2]$.[84−86] The reaction chemistry of these two compounds, however, differs significantly from that of the (μ-hydroxo)diiron complexes discussed above. The postulated mechanism[84] involves oxidation of the diiron(II) compound by dioxygen to generate a putative peroxo $\{Fe^{III}_2(O_2^{2-})\}^{4+}$ or bis(μ-oxo) $\{Fe^{IV}_2(O^{2-})_2\}^{4+}$ intermediate, which reacts rapidly with a second equivalent of the initial diiron(II) complex to afford equimolar mixtures of valence-delocalized $Fe^{II}Fe^{III}$ and valence-trapped $Fe^{III}Fe^{IV}$ species.

Oxidative *N*-Dealkylation Effected by 4. Compound **4** rapidly reacts with dioxygen in CH_2Cl_2 to yield a brown solution that exhibits a broad feature extending across the entire visible region. Similar spectra were observed over a wide temperature range (−78 to 23 °C) and also by addition of H_2O_2 to a solution of **4** in MeCN (−40 to 23 °C). The recent observation of oxidative *N*-dealkylation of activated benzyl groups in the complex $[Fe_2(\mu\text{-}O_2CAr^{Tol})_4(N,N\text{-}Bn_2\text{-}en)_2]$ following exposure to dioxygen[39,87] led us to analyze solutions of **4** + O_2 for ligand oxidation. GC−MS analysis revealed that benzaldehyde was indeed generated by oxidation of **4**. With O_2 in CH_2Cl_2, PhCHO formed in 30% yield relative to **4**, and a 51% yield was obtained when H_2O_2 in MeCN was employed.

The ability of **4** to promote the oxidation of external substrates was also examined. Gentle purging by dioxygen of a CH_2Cl_2 solution of **4** and bis(4-methylbenzyl)amine yielded both PhCHO and tolualdehyde in a ratio of ~1:1. When the reaction was performed using H_2O_2 in MeCN, a copious amount of precipitate formed; analysis of the reaction mixture by GC and GC−MS was precluded by similar retention times of tolualdehye and the other products that formed. Other substrates were screened: PPh_3 did not convert to Ph_3PO nor did oxidation of 9,10-dihydroanthracene afford anthracene. Use of 2,4-di-*tert*-butylphenol did not generate the corresponding biphenol, although the solution dramatically changed color to dark blue, most likely the result of a phenoxide-to-iron(III) charge-transfer band.[88] The coordination of the phenol to the iron center was accompanied by a substantial decrease in PhCHO production (O_2, 7%; H_2O_2, 39%). Taken together, these results suggest that the oxidation chemistry does not proceed by a simple hydrogen atom abstraction mechanism and that the amine oxidation is not due to an organic radical.

Comparison of Substrate Oxidation by 4 and 5. The relatively inefficient yield of tolualdehyde by **4** led us to study the oxidation chemistry of compound **5**. Replacement of the pendant benzyl groups of the BBAN ligand of **4** with the ethyl groups of BEAN was expected to eliminate oxidative *N*-dealkylation of the ligand framework due to the significantly stronger (12 kcal/mol) C−H bonds of the ethyl substituents.[89] We hypothesized that elimination of ligand oxidation might lead to higher yields for the oxidation of external substrates, owing to diminished competition from an internal ligand fragment.

Reaction of **5** with dioxygen in CH_2Cl_2 afforded a brown solution with a broad feature in the optical spectrum, similar to that observed for **4**. Analysis of the reaction mixture by GC revealed no acetaldehyde, a product that would form following *N*-dealkylation. This conclusion was confirmed by a colorimetric test for CH_3CHO,[90] which similarly gave a negative result. Acid decomposition of the oxidized species, followed by analysis using ^{1}H NMR spectroscopy, showed the BEAN ligand to be intact, with no indication that hydroxylation of the ethyl groups had occurred. Exposure of a solution of **5** and bis(4-methylbenzyl)amine to dioxygen afforded tolualdehyde in only ~0.8%. A possible explanation for this low yield is that a carboxylate shift is required to allow approach of the amine to the iron centers. In the absence of such a structural change, the amine cannot easily access the iron sites of **5** and formation of aldehyde is negligible.

(78) Payne, S. C.; Hagen, K. S. *J. Am. Chem. Soc.* **2000**, *122*, 6399−6410.
(79) Nivorozhkin, A. L.; Anxolabéhère-Mallart, E.; Mialane, P.; Davydov, R.; Guilhem, J.; Cesario, M.; Audière, J.-P.; Girerd, J.-J.; Styring, S.; Schussler, L.; Seris, J.-L. *Inorg. Chem.* **1997**, *36*, 846−853.
(80) Mizoguchi, T. J.; Kuzelka, J.; Spingler, B.; DuBois, J. L.; Davydov, R. M.; Hedman, B.; Hodgson, K. O.; Lippard, S. J. *Inorg. Chem.* **2001**, *40*, 4662−4673.
(81) Mizoguchi, T. J.; Davydov, R. M.; Lippard, S. J. *Inorg. Chem.* **1999**, *38*, 4098−4103.
(82) Davydov, R. M.; Ménage, S.; Fontecave, M.; Gräslund, A.; Ehrenberg, A. *J. Biol. Inorg. Chem.* **1997**, *2*, 242−255.
(83) Bossek, U.; Hummel, H.; Weyhermüller, T.; Bill, E.; Wieghardt, K. *Angew. Chem., Int. Ed. Engl.* **1995**, *34*, 2642−2645.
(84) Lee, D.; Pierce, B.; Krebs, C.; Hendrich, M. P.; Huynh, B. H.; Lippard, S. J. *J. Am. Chem. Soc.* **2002**, *124*, 3993−4007.
(85) Lee, D.; DuBois, J. L.; Pierce, B.; Hedman, B.; Hodgson, K. O.; Hendrich, M. P.; Lippard, S. J. *Inorg. Chem.* **2002**, *41*, 3172−3182.
(86) Lee, D.; Du Bois, J.; Petasis, D.; Hendrich, M. P.; Krebs, C.; Huynh, B. H.; Lippard, S. J. *J. Am. Chem. Soc.* **1999**, *121*, 9893−9894.
(87) Lee, D.; Lippard, S. J. *J. Am. Chem. Soc.* **2001**, *123*, 4611−4612.
(88) Gaber, B. P.; Miskowski, V.; Spiro, T. G. *J. Am. Chem. Soc.* **1974**, *96*, 6868−6873.
(89) March, J. In *Advanced Organic Chemistry*, 4th ed.; John Wiley & Sons: New York, 1992; p 191.
(90) Feigl, F. In *Spot Tests in Organic Analysis*; Elsevier Publishing Co.: New York, 1960; pp 352−353.

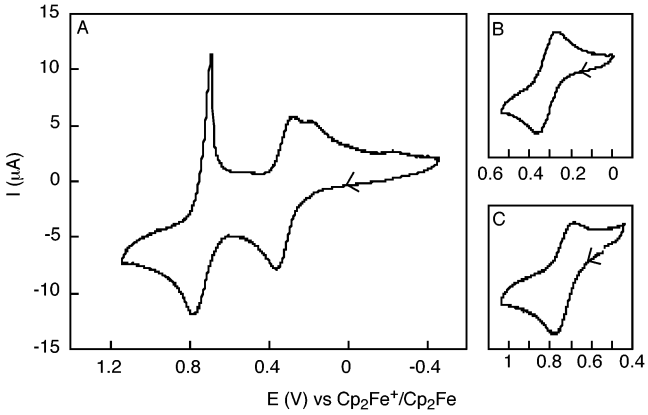

Figure 6. Cyclic voltammograms of 2 mM $[Fe_2(BPMAN)(\mu\text{-}O_2CPh)_2](OTf)_2$ (**1**) in CH_2Cl_2 with 0.5 M $Bu_4N(PF_6)$ as supporting electrolyte with applied potentials of +1.2 to −0.4 V (scan rate = 100 mV/s) (A), +0.5 to 0 V (scan rate = 200 mV/s) (B), and +1 to +0.4 V (scan rate = 200 mV/s) (C), vs Cp_2Fe^+/Cp_2Fe.

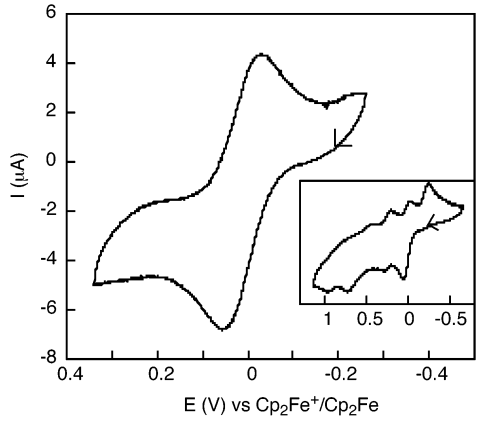

Figure 7. Cyclic voltammograms of 2 mM $[Fe_2(BPMAN)(\mu\text{-}OH)(\mu\text{-}O_2CAr^{Tol})](OTf)_2$ (**2**) in CH_2Cl_2 with 0.5 M $Bu_4N(PF_6)$ as supporting electrolyte and a scan rate of 100 mV/s. The insert shows the CV recorded when potentials greater than +0.4 V vs Cp_2Fe^+/Cp_2Fe were applied.

Electrochemical Studies. Cyclic voltammograms (CVs) of compounds **1**, **2**, and **4** in CH_2Cl_2 were recorded to study their relative ease of oxidation. The CV of the bis(μ-carboxylato) complex **1**, shown in Figure 6, reveals two reversible redox waves with $E_{1/2}$ values of +310 mV (ΔE_p = 80 mV) and +733 mV (ΔE_p = 94 mV) vs Cp_2Fe^+/Cp_2Fe, corresponding to the $Fe^{III}Fe^{II}/Fe^{II}Fe^{II}$ and $Fe^{III}Fe^{III}/Fe^{III}Fe^{II}$ couples, respectively. These redox waves are reversible only when each is studied in isolation; irreversible behavior occurs on the return reduction scan when the two oxidation sweeps are carried out consecutively. The unusually sharp peak on the return scan probably indicates compound decomposition or adsorption to electrode. The related compound $[Fe_2(BPMAN)(\mu\text{-}O_2CPhCy)_2](OTf)_2$, which has $E_{1/2}$ values of +296 mV (ΔE_p = 80 mV) and +781 mV (ΔE_p = 74 mV), was the first carboxylate-bridged diiron(II) complex without an additional single atom bridge to exhibit two, rather than just one, reversible redox waves.[23] Probably, the larger $PhCyCO_2^-$ ligands are better able to stabilize the $Fe^{III}Fe^{II}/Fe^{II}Fe^{II}$ and $Fe^{III}Fe^{III}/Fe^{III}Fe^{II}$ couples than the benzoate groups of **1**.

The CV of the (μ-hydroxo)(μ-carboxylato) compound **2**, presented in Figure 7, shows a reversible redox wave with an $E_{1/2}$ value of +11 (ΔE_p = 82 mV) vs Cp_2Fe^+/Cp_2Fe when potentials less than 400 mV are applied. As observed with $[Fe_2(BPMAN)(\mu\text{-}OH)(\mu\text{-}O_2CPhCy)](OTf)_2$,[23] higher potentials caused the reduction wave to split into three components. The redox potential of **2** is 33 mV above that of the $PhCyCO_2^-$ derivative, consistent with aromatic ligands being less donating than alkyl groups, and 299 mV below that of **1**, reflecting the more donating nature of the hydroxide unit.

The CV of the paddle-wheel compound **4** displays irreversible oxidation at potentials above +1000 mV vs Cp_2Fe^+/Cp_2Fe. This result can be compared to the irreversible electrochemistry exhibited by $[Fe_2(BEAN)(\mu\text{-}O_2CPhCy)_3](OTf)$ at potentials above +400 mV[23] and the reversible behavior of $[Fe_2(\mu\text{-}O_2CAr^{Tol})_4(4\text{-}^tBuC_5H_4N)_2]$ ($E_{1/2}$ = −216 mV).[91] The studies with $[Fe_2(BEAN)(\mu\text{-}O_2CPhCy)_3](OTf)$ made clear the need for a fourth carboxylate ligand to stabilize a diiron(II,III) species in compounds with these paddle-wheel motifs. The significant difference in oxidation potential between **4** and $[Fe_2(BEAN)(\mu\text{-}O_2CPhCy)_3](OTf)$ ($\Delta E_{1/2}$ = 600 mV) is consistent with the more electron-withdrawing ligand environment of **4**, but because the processes are irreversible, a more quantitative explanation cannot be offered. Unlike **4**, $[Fe_2(BEAN)(\mu\text{-}O_2CPhCy)_3](OTf)$ is not sensitive to dioxygen, but this property probably is not due to electronic differences because the opposite behavior would be expected based on $E_{1/2}$ values.

Discussion

The naphthyridine moiety of the ligands BPMAN, BBAN, and BEAN can be viewed as a "masked carboxylate," because the two units bridge metal ions in an analogous manner. In particular, both moieties facilitate the synthesis of dimetallic compounds that feature the μ-1,3-coordination mode found at the active sites of carboxylate-bridged dinuclear metalloproteins. The multidentate nature of the naphthyridine ligands, afforded by appendages that are readily installed and positioned to coordinate to the bridged dimetallic center, ensure that a dinuclear core is maintained not only in the diiron(II) starting compounds, but also in their subsequent oxidation products. This property is much more difficult to achieve with substituted carboxylate ligands. By varying both the naphthyridine fragment and the ancillary ligands, a variety of diiron(II) compounds was prepared. Use of the relatively compact benzoate unit in conjunction with the octadentate BPMAN ligand afforded the bis(μ-carboxylato)diiron(II) core of complex **1**. Such a species cannot be accommodated with the sterically demanding $Ar^{Tol}CO_2^-$ ligand, and when this ligand is employed, only one bridging carboxylate group is encountered. The resulting complexes **2** and **3** incorporate as their third bridging ligand the less sterically demanding single-atom hydroxide and methoxide groups, respectively. When the tetradentate ligands BBAN and BEAN were employed, the paddle-wheel compounds **4** and **5** were readily assembled. In addition to promoting the quadruply-bridged core of these complexes, BBAN and

(91) Lee, D.; Krebs, C.; Huynh, B. H.; Hendrich, M. P.; Lippard, S. J. *J. Am. Chem. Soc.* **2000**, *122*, 5000−5001.

BEAN also serve to bring potential substrates, benzyl and ethyl substituents, respectively, into close proximity to the diiron core.

The electrochemical properties of the naphthyridine-based diiron(II) complexes reflect the expected trend of ligands bearing electron-donating substituents, which convey lower redox potentials. A comparison of the cyclic voltammograms of **1** and the related compound $[Fe_2(BPMAN)(\mu\text{-}O_2CPhCy)_2](OTf)_2$[23] reveals the latter to have a more reversible second oxidation wave, which may imply that the higher oxidation state is better stabilized by bulkier ligands. If so, it suggests a design strategy for future synthetic work aimed at accessing higher oxidation level diiron complexes. In general, the compounds exhibiting low redox potentials react with dioxygen or H_2O_2 more readily than those with higher oxidation values. Complex **4**, however, is more reactive toward O_2 despite its high redox potential, which we attribute to the need for a carboxylate shift.

The dinucleating nature of the 1,8-naphthyridine-based ligands allowed the reactivity of compounds **1**−**5** to be probed within an environment constrained to enforce dimetallic character. This feature is important because the related non-heme diiron enzymes more rigorously maintain dinuclear cores. In contrast, the nuclearity or ligand composition of active oxidants in model systems that display substrate oxidation is often uncertain.[92−94] The oxidation of compounds **1**−**3** to afford (μ-oxo)diiron(III) and (μ-oxo)Fe(II)Fe(III) species mirrors well-documented reactivity between Fe(II) compounds and dioxygen. Although oxidation of mononuclear iron(II) compounds to afford oxo-bridged diiron(III) units can occur,[95−97] in the present case we can rule out such a pathway owing to the dinucleating nature of the ligands.

Oxidative *N*-dealkylation of the benzyl groups of the BBAN ligand or of added bis(4-methylbenzyl)amine to form PhCHO and tolualdehyde, respectively, was observed in the reaction of **4** with dioxygen or H_2O_2. Such reactivity is common with iron porphyrins,[98] but in non-heme diiron systems it is limited to the reaction of $[Fe_2(\mu\text{-}O_2CAr^{Tol})_4(N,N\text{-}Bn_2en)_2]$ with dioxygen.[39,87] Oxidative *N*-dealkylation of **4** is thus a worthy addition to the emerging class of diiron compounds displaying this chemistry. Consistent with the stronger C−H bonds of the ethyl substituents of BEAN in **5**, *N*-dealkylation with this compound was not observed.

Conclusions

A major aim of this work was to delineate the requirements for accessing O_2-activating non-heme diiron(II) compounds of controlled nuclearity. Although the 1,8-naphthyridine-based ligands employed in this study did not allow the detection of $\{Fe_2(O)_2\}$ adducts, the dinuclear structures of both the starting diiron(II) compounds and the oxidized products were kinetically controlled by the multidentate ligand scaffolds. Enhanced dioxygen reactivity was achieved by introduction of electron-donating or coordinately flexible ligands. Inner-sphere reactions between the diiron core and dioxygen are implied, and carboxylate ligands are good candidates to promote this reaction because of their ability to adopt different coordinate modes in order to allow access to the iron centers.

The activation of C−H bonds, the ultimate goal in modeling non-heme diiron enzymes, requires the substrate to be in close proximity to the active $\{Fe_2(O)_2\}$ oxidant. The studies with compound **4** show that an intermediate can be intercepted by appending the substrate to the supporting ligand scaffold, thus promoting accessibility to the diiron core. This strategy, therefore, suggests a viable route for achieving efficient activation of C−H bonds by diiron compounds. In the related non-heme diiron enzymes, the dinuclear core is proximal to a substrate-binding cavity. The design and construction of such a feature into future ligand frameworks remains an important future objective for the preparation of fully functional model compounds.

Acknowledgment. This work was supported by grants from the National Science Foundation and National Institute of General Medical Sciences. J.K. is a NSERC predoctoral fellow. B.S. thanks the Swiss National Science Foundation for support. We are grateful to Dr. Mu-Hyun Baik for sharing unpublished results of DFT calculations on **2**, Dr. Weiming Bu for assistance with crystallographic analyses, Mr. Sungho Yoon for help in acquiring the Mössbauer spectra, and Ms. Li Li of the MIT Department of Chemistry Instrumentation Facility for performing the ESI-MS measurements of compounds **2** and **3**.

Supporting Information Available: Scan rate plots for the electrochemistry of **1** and **2** in Figures S1 and S2, Mössbauer spectra of the final oxidation products of **1** and **2** in Figure S3, the full numbering schemes of compound **1**, **3**, **4**, and **5** in Figures S4−S7, and data tables for the subject compounds (PDF), and X-ray crystallographic files for these compounds in CIF format. This material is available free of charge via the Internet at http://pubs.acs.org.

IC0345976

(92) Moll, N. R.-P. Y.; Banse, F.; Miki, K.; Nierlich, M.; Girerd, J.-J. *Eur. J. Inorg. Chem.* **2002**, 1941−1944.
(93) Okuno, T.; Ito, S.; Ohba, S.; Nishida, Y. *J. Chem. Soc., Dalton Trans.* **1997**, 3547−3551.
(94) Ménage, S.; Vincent, J. M.; Lambeaux, C.; Chottard, G.; Grand, A.; Fontecave, M. *Inorg. Chem.* **1993**, *32*, 4766−4773.
(95) Balland, V.; Banse, F.; Anxolabéhère-Mallart, E.; Ghiladi, M.; Mattioli, T. A.; Philouze, C.; Blondin, G.; Girerd, J.-J. *Inorg. Chem.* **2003**, *42*, 2470−2477.
(96) Enomoto, M.; Aida, T. *J. Am. Chem. Soc.* **2002**, *124*, 6099−6108.
(97) Kitajima, N.; Tamura, N.; Amagai, H.; Fukui, H.; Moro-oka, Y.; Mizutani, Y.; Kitagawa, T.; Mathur, R.; Heerwegh, K.; Reed, C. A.; Randall, C. R.; Que, L., Jr.; Tatsumi, K. *J. Am. Chem. Soc.* **1994**, *116*, 9071−9085.
(98) Sono, M.; Roach, M. P.; Coulter, E. D.; Dawson, J. H. *Chem. Rev.* **1996**, *96*, 2841−2887.